

Dectin-1 Agonist, Curdlan, Regulates Osteoclastogenesis by Inhibiting Nuclear Factor of Activated T-cells Cytoplasmic 1 through Syk Kinase*

Toru Yamasaki^{1,2}, Wataru Ariyoshi¹, Toshinori Okinaga¹, Yoshiyuki Adachi³, Ryuji Hosokawa², Shinichi Mochizuki⁴, Kazuo Sakurai⁴ and Tatsuji Nishihara¹

¹From the Division of Infections and Molecular Biology, Department of Health Promotion, Kyushu Dental University, Kitakyushu, Fukuoka 803-8580, Japan

²Division of Oral Reconstruction and Rehabilitation, Department of Oral Functions, Kyushu Dental University, Kitakyushu, Fukuoka 803-8580, Japan

³Laboratory for Immunopharmacology of Microbial Products, School of Pharmacy, Tokyo University of Pharmacy and Life Sciences, Hachioji, Tokyo 192-0392, Japan

⁴Department of Chemistry and Biochemistry, The University of Kitakyushu, Kitakyushu, Fukuoka 808-0135, Japan

*Running title: *Curdlan Regulates Osteoclastogenesis by Dectin-1*

To whom correspondence should be addressed: Wataru Ariyoshi, Division of Infections and Molecular Biology, Department of Health Promotion, Kyushu Dental University, 2-6-1 Manazuru, Kokurakita-ku, Kitakyushu, Fukuoka, Japan, [REDACTED]

Keywords: Bone marrow; Differentiation; NFAT transcription factor; Nuclear Translocation; Osteoclast; Pattern recognition receptor; Curdlan; Dectin-1; Syk; c-fos

Background: Dectin-1 is found on myeloid lineage cells and contains an immunoreceptor tyrosine-based activation motif, from which signals are associated with bone homeostasis.

Results: Dectin-1 agonist, curdlan, suppresses osteoclastogenesis induced by receptor activator of nuclear factor- κ B ligand (RANKL).

Conclusion: Curdlan regulates RANKL-induced osteoclastogenesis.

Significance: Curdlan could be a potential therapeutic candidate in treating osteoclast-related diseases.

ABSTRACT

Several immune system cell-surface receptors are reported to be associated with osteoclastogenesis. Dectin-1, a lectin receptor for β -glucan, is found predominantly on cells of the myeloid lineage. In the present study, we examined the effect of dectin-1 agonist, curdlan, on osteoclastogenesis. In mouse bone marrow cells (BMCs) and dectin-1 over-expressing RAW 264.7 cells (d-RAWs), curdlan suppressed receptor activator of nuclear factor- κ B (NF- κ B) ligand (RANKL)-induced

osteoclast differentiation, bone resorption and actin-ring formation, in a dose-dependent manner. This was achieved within non-growth inhibitory concentrations at the early stage. Conversely, curdlan had no effect on macrophage colony-stimulating factor (M-CSF)-induced differentiation. Furthermore, curdlan inhibited RANKL-induced nuclear factor of activated T-cell cytoplasmic 1 (NFATc1) expression, thereby decreasing osteoclastogenesis-related marker gene expression, including tartrate-resistant acid phosphatase (TRAP), osteoclast stimulatory transmembrane protein (OC-STAMP), cathepsin K and matrix metalloproteinase 9 (MMP-9). Curdlan inhibited RANKL-induced c-fos expression, followed by suppression of NFATc1 autoamplification, without significantly affecting the NF- κ B signaling pathway. We also observed that curdlan treatment decreased Syk protein in d-RAWs. Inhibition of the dectin-1-Syk kinase pathway, by Syk-specific siRNA or chemical inhibitors, suppressed osteoclast formation and NFATc1 expression stimulated by RANKL. In

conclusion, our results demonstrate that curdlan potentially inhibits osteoclast differentiation, especially NFATc1 expression, and that Syk kinase plays a crucial role in the transcriptional pathways. This suggests activation of dectin-1-Syk kinase interaction critically regulates the genes required for osteoclastogenesis.

Osteoclasts originate from hematopoietic precursors of the monocyte/macrophage lineage, which differentiate into multinucleated, giant cells, specialized to resorb bone by fusion of mononuclear progenitors (1). Osteoclasts are unique in their ability to resorb bone, and play an important role in regulating bone remodeling. Osteoclast precursors interact with osteoblasts and stromal cells to permit their differentiation into mature osteoclasts (2). Furthermore, osteoclast formation is induced in the presence of RANKL, a member of the TNF superfamily, expressed by osteoblasts and bone stromal cells. RANKL interacts with the osteoclast cell surface receptor, RANK, which in turn recruits cytosolic TNF receptor-associated factors (TRAFs) (3), prior to activation of downstream signaling pathways. These signaling pathways include, extracellular signal-regulated kinase (ERK), p38 MAPK, NF- κ B and activator protein-1 (AP-1), including c-jun and c-fos. Finally, expression of the nuclear factor of activated T-cell cytoplasmic 1 (NFATc1), a key molecule for osteoclastogenesis, is induced (4).

Pattern recognition receptors (PRRs) recognize molecular signatures of microbes and play an important role in initiation of immune responses to infection (5). Dectin-1 is a type II membrane receptor, containing a single extracellular C-type lectin-like domain (6) and an immunoreceptor tyrosine-based activation motif (ITAM) in the cytoplasmic tail (7). Dectin-1 is found on cells of the myeloid lineage, including monocytes, macrophages, neutrophils, dendritic cells and a subset of T cells, in mice (8). It has been shown that dectin-1 is a major receptor for the recognition of β -1, 3-linked and/or β -1, 6-linked glucans (β -glucans) (8, 9).

Dectin-1 is known to mediate its own signaling through its cytoplasmic tail (10), and tyrosine residues within its receptor ITAM motif are phosphorylated by Src family tyrosine kinases through engagement with dectin-1. This is followed by recruitment and activation of Syk, nonreceptor tyrosine kinase (11-13), with activation of several intracellular signaling

pathways, including NF- κ B, MAPK and NFAT (14).

The β -glucans, consisting of a backbone of polymerized β -(1, 3)-linked β -D-glucopyranosyl units and β -(1, 6)-linked side chains, are a major cell component of fungi and also found in plants and some bacteria (15). They are known to possess anti-infection and anti-tumorigenic properties, by possessing the ability to activate leukocytes in stimulating their phagocytic activity, the production of reactive oxygen intermediates and inflammatory mediators, including TNF- α (16-19). However, the mechanism of β -glucan-induced activity has not been elucidated precisely because pathogen-derived components are often contaminated by β -glucan preparations. Recently, curdlan, a linear nonionic homopolymer of D-glucose with (1, 3) glucosidic linkages, has been identified as a dectin-1 specific agonist and has gained attention from the pharmaceutical industry as an immunomodulatory drug delivery vehicle (20, 21).

Several cell-surface receptors in the immune system are reported to be associated with osteoclastogenesis. ITAM-dependent co-stimulatory signals, activated by multiple immunoreceptors, are essential for the maintenance of bone homeostasis (22). It has been demonstrated that Syk modulates osteoclast function *in vitro* and *in vivo* (23-25). However, the direct effects of β -glucans on osteoclastogenesis are largely unknown. In the present study, we examined the effect of curdlan, a linear homopolymer of D-glucose, on osteoclastogenesis. We also identified the precise mechanisms by which curdlan suppresses osteoclast formation *in vitro*.

EXPERIMENTAL PROCEDURES

Reagents and antibodies – Curdlan was purchased from Wako Pure Chemical Industries (Osaka, Japan) and diluted with 0.1 N NaOH. Anti-NFATc1 polyclonal antibody, anti-I κ B- α polyclonal antibody and anti-RANK polyclonal antibody were obtained from Santa Cruz Biotechnology (Santa Cruz, CA, USA) and anti- β -actin monoclonal antibody was purchased from Sigma-Aldrich (St. Louis, MO, USA). Anti-c-fos monoclonal antibody, anti-Syk polyclonal antibody, anti-phospho-Syk monoclonal antibody, anti-c-jun monoclonal antibody, anti-phospho-c-jun monoclonal antibody, and anti-Histone H3 monoclonal antibody were purchased from Cell Signaling

Technology Inc. (Beverly, MA, USA). Anti-dectin-1 polyclonal antibody was purchased from R&D Systems (Minneapolis, MN, USA).

Cell culture – Bone marrow cells (BMCs) were isolated from femurs and tibias of 6-week-old male ddY mice (Kyudo Co, Ltd, Saga, Japan) and maintained in α -minimum essential medium (α -MEM; GIBCO, Grand Island, NY, USA) supplemented with 10% fetal calf serum (FCS, Sigma-Aldrich), 100 U/ml penicillin G Potassium Salt (Nacalai tesque, Kyoto, Japan) and 100 μ g/ml streptomycin (Wako Pure Chemical Industries). Cells (4×10^4) were cultured with M-CSF (20 ng/ml; Peprotech Rocky Hill, NJ, USA) and RANKL (40 ng/ml; Peprotech), in the presence or absence of curdlan, on 48-well plates at 37°C in 5% CO₂ for 4 days, to generate mature osteoclasts. All procedures were approved by the Animal Care and Use Committee of the Kyushu Dental University.

In order to prepare dectin-1 retrovirus vector, cDNA-encoded mouse dectin-1 was cloned into pFB-Neo plasmid (Agilent Technologies, Inc. Santa Clara, CA, USA). GP2-293 packaging cells (Clontech Laboratories, Inc., Mountain View, CA, USA) were transfected by the plasmid mixture containing dectin-1/pFB-Neo and pVSV-G (Clontech Laboratories, Inc.) with Lipofectamine LTX (Invitrogen, Grand Island, NY, USA) in accordance with the manufacturer's protocol. The culture supernatant of GP2-293 cells was harvested as a retrovirus fluid for dectin-1 transfection. RAW 264.7 cells (RIKEN cell bank, Tsukuba, Japan) were cultured with the virus vector in the presence of polybrene 8 μ g/ml for 48 h. Cells expressing dectin-1 (d-RAW) were maintained in α -MEM containing 10% FCS, penicillin G (100 U/ml), streptomycin (100 μ g/ml), and G418 Disulfate Aqueous Solution (50 mg/ml; Nacalai tesque). For the negative control of d-RAW, control virus vector without dectin-1 cDNA was used for infection (c-RAW). Expression of dectin-1 molecules on RAW 264.7 cells was examined by antibody staining using anti-mouse dectin-1 (Clone RH1; BioLegend, San Diego, CA, USA). Cells (1×10^3 cells/well) were cultured for 7 days with RANKL (40 ng/ml), in the presence or absence of curdlan, on 96-well plates at 37°C in 5% CO₂, to generate mature osteoclasts. In some experiments, cells were treated with selective inhibitor of Syk kinase, piceatannol (Calbiochem, San Diego, CA, USA) and BAY 61-3606 (Calbiochem) for 1 h, prior to stimulation with RANKL, in the presence or

absence of each inhibitor. Mouse bone marrow stromal cells, ST2, were obtained from Riken Cell Bank (Ibaraki, Japan) and maintained in α -MEM supplemented with 10% FCS, 100 U/ml penicillin G, and 100 mg/ml streptomycin at 37°C in an atmosphere of 5% CO₂.

Evaluation of osteoclast differentiation – After culture, adherent cells were fixed and stained with TRAP using a leukocyte acid phosphatase kit (Sigma-Aldrich). TRAP-positive multinucleated cells, containing three or more nuclei, were considered to be osteoclasts and were counted using a microscope.

Assessment of actin ring formation – Mature osteoclasts were prepared from BMCs by treatment with M-CSF (20 ng/ml) and RANKL (40 ng/ml) in the presence or absence of curdlan for 5 days on 8-well chamber slides (Thermo Fisher Scientific, Waltham, MA, USA). In some experiments, d-RAWs were cultured for 8 days with RANKL (40 ng/ml) in the presence or absence of curdlan for 8 days on the chamber slides. Cells were fixed with 4% paraformaldehyde (PFA) in PBS for 60 min at 4°C, quenched with 0.2 M glycine in PBS, and permeabilized using 0.2% Triton X-100 for 10 min at room temperature (r.t). After washing in PBS, cells were incubated with Alexa Fluor 488-phalloidin (Invitrogen) for 60 min at r.t, then washed, mounted in mounting media containing nuclear DAPI stain (Vector Laboratories Inc., Burlingame, CA, USA) and visualized using Fluorescence Microscope BZ-9000 (Keyence Corp., Osaka, Japan). Images were captured digitally in real-time and processed using BZ-II imaging software (Keyence Corp.).

Assessment of bone resorption – For the bone resorption assay, BMCs were cultured for 7 days with M-CSF (20 ng/ml) and RANKL (40 ng/ml) in the presence or absence of curdlan, on an Osteo Assay Stripwell Plate® (Corning Inc., NY, USA). d-RAWs were cultured for 10 days with RANKL (40 ng/ml) in the presence or absence of curdlan. To quantitate resorption lacunae, cells were removed by 5% sodium hypochlorite, followed by extensive washing with distilled water and air drying. In some experiments for pit assay, BMCs were cultured with M-CSF (20 ng/ml) and RANKL (40 ng/ml) in the presence or absence of curdlan, on dentin slices (Wako Pure Chemical Industries). Cells on dentin slices were removed and pits were stained with Mayer's Hematoxylin Solution (Muto Pure Chemicals Co, Ltd, Tokyo, Japan). The absorbed areas on the discs and dentin

slices were observed under a microscope and quantified using ImageJ software (NIH Image, National Institutes of Health; online at <http://rsb.info.nih.gov>).

Quantitative real-time RT-PCR – Total RNA was isolated from cells with the RNeasy Mini Kit (QIAGEN Inc., Valencia, CA, USA), according to the manufacturer's instructions. RNA was transcribed with q-Script cDNA Supermix reagents (Quanta BioSciences, Gaithersburg, MD, USA) and amplified for 30 min at 42°C. For real-time RT-PCR, PCR products were detected using FAST SYBR® Green Master Mix (Applied Biosystems, Foster City, CA, USA) using the following primer sequences: *gapdh* forward; 5'-GACGGCCGCATCTTCTTGA-3' and reverse; 5'-CACACCGACCTTCACCATTTT-3', *dectin-1* forward; 5'-CCTTGGAGGCCATTGC-3' and reverse; 5'-GCAACCACTACTACCACAAAGCA-3', *nfatc1* forward; 5'-ACCACCTTCCGCAACCA-3', and reverse; 5'-GGTACTGGCTTCTCTCCGTTTC-3', *trap* forward; 5'-CTGCTGGGCCTACAAATCATA-3', and reverse; 5'-GGGAGTCCTCAGATCCATAGT-3' *oc-stamp* forward; 5'-CCGCAGCCTGACATTTGAG-3', and reverse; 5'-TCTCCTGAGTGATCGTGTGCAT-3', *cathepsin k* forward; 5'-TATGACCACTGCCTTCAATAC-3', and reverse; 5'-GCCGTGGCGTTATACATACA-3', *mmp9* forward; 5'-TGAGCTGGACAGCCAGACTAAA-3', and reverse; 5'-TCGCGGCAAGTCTTCAGAGTAGTT-3'.

Thermal cycling and fluorescence detection were performed using a StepOne™ Real-Time System (Applied Biosystems). Relative changes in gene expression were calculated using the comparative CT method. Total cDNA abundance between samples was normalized using primers specific to the GAPDH gene.

Immunoblot analysis – Total protein was extracted using Cell Lysis Buffer (Cell Signaling Technology) containing a protease inhibitor cocktail (Thermo Fisher Scientific) and a phosphatase inhibitor cocktail (Nacalai tesque). Protein contents were measured using a DC protein assay kit (Bio-Rad, Hercules, CA, USA). Total protein (20 µg/sample) was loaded and separated on a 10–20% e-PAGEL (ATTO Corp., Tokyo, Japan), then transferred to PVDF membranes (Millipore Corp., Bedford, MA, USA). Non-specific binding sites were blocked for 30 min by immersing the membrane in Blocking One (Nacalai Tesque) at r.t. Membranes were subjected to overnight incubation with diluted primary antibodies at 4°C, followed by HRP

conjugated secondary antibodies for 60 min at r.t. HRP-conjugated anti-mouse and anti-rabbit IgG were used as secondary antibodies (GE Healthcare, Little Chalfont, UK). After washing the membranes, chemiluminescence was produced using ECL reagent (Amersham Pharmacia Biotech, Uppsala, Sweden) or Chemi-Lumi One Super (Nacalai tesque) and detected digitally with GelDoc XR Plus (Bio-Rad).

Nuclear Translocation of NFATc1 – d-RAWs were cultured with or without curdlan (25 µg/ml) in the presence of RANKL (40 ng/ml) for 6 h. Cultured cells were harvested and collected by centrifugation at 300 × g for 5 min, and cell pellets were treated with NE-PER Nuclear and Cytoplasmic Extraction Reagents (Thermo Scientific) according to the manufacturer's instructions. Cell fractions were subjected to SDS-PAGE and immunoblotted with antibody against NFATc1 antibody. In other experiments, d-RAWs were cultured with or without curdlan (25 µg/ml) in the presence of RANKL (40 ng/ml) for 3 h in 8-well chamber slides. Treated cells were fixed in 4% PFA in PBS for 60 min at 4°C and quenched with 0.2 M glycine in PBS. Cells were permeabilized using 0.2% Triton X-100 for 10 min at r.t, followed by blocking with 1% bovine serum albumin (BSA, Sigma-Aldrich) in PBS for 30 min. After washing in PBS, cells were incubated with anti-NFATc1 (2.0 µg/ml) antibody for 60 min at r.t. After washing in PBS, cells were incubated with Alexa Fluor 488 conjugated anti-mouse secondary antibody (Invitrogen), then washed, mounted in mounting media containing DAPI and visualized using Fluorescence Microscope BZ-9000. Images were captured digitally in real-time and processed using BZ-II imaging software.

Immunofluorescence analysis of Syk – d-RAWs were cultured with or without curdlan (25 µg/ml) for the indicated times in 8-well chamber slides. Treated cells were fixed in 4% PFA in PBS for 60 min at 4°C and quenched with 0.2 M glycine in PBS. Cells were permeabilized using 0.2% Triton X-100 for 10 min at r.t, followed by blocking with 1% BSA in PBS for 30 min. After washing in PBS, cells were incubated with anti-Syk polyclonal antibody (Santa Cruz, 2.0 µg/ml) overnight at 4°C. After washing in PBS, cells were incubated with Alexa Fluor 488 conjugated anti-rabbit secondary antibody (Invitrogen), then washed, mounted in mounting media containing DAPI and visualized using Fluorescence Microscope BZ-9000 (Keyence

Corp.). Images were captured digitally in real-time and processed using BZ-II imaging software.

Silencing of Syk expression by specific siRNA – siRNA targeting was used to knockdown Syk expression in d-RAWs. siRNA against mouse Syk and siRNA were purchased from Santa Cruz Biotechnology. NEPA21 Super Electroporator (Nepa Gene Co., Ltd., Chiba, Japan) was used to deliver siRNA into cells according to the manufacturer's instructions. In brief, 1.0×10^6 cells were suspended in 100 μ l of α -MEM and transfected with siRNA at a final concentration of 300 nM. Transfected cells were immediately diluted with pre-warmed α -MEM and cultured in 6-well plates for 24 h before stimulation with RANKL. Specific gene knockdowns were assessed by real-time RT-PCR.

Statistical analyses – All data were obtained from three independent experiments and each experiment was performed in triplicate. Statistical analyses were carried out using JMP[®] software, version 10.0.2 (SAS Institute Inc., Cary, NC, USA). All data were expressed as mean \pm standard deviation and analyzed by one-way analysis of variance (ANOVA) followed by a suitable post-test (Dunnett's or Tukey's) or Student's *t* test. *P* values of less than 0.05 were considered statistically significant.

RESULTS

Curdlan inhibits osteoclast formation and function in BMCs – To determine whether curdlan affects osteoclast differentiation, we first evaluated osteoclast number by counting TRAP-positive multinucleated cells. Curdlan inhibited differentiation of BMCs into osteoclast-like cells, mediated by M-CSF and RANKL. As shown in Fig. 1A and 1B, the effect of curdlan was dose-dependent, with maximum inhibition observed at a concentration of 50 μ g/ml (91.1% inhibition). Differentiated mature osteoclasts can resorb the mineral substratum on discs coated with calcium phosphate, as well as dentin slices (26-28). To determine whether curdlan affects osteoclast function, differentiated BMCs were cultured on an Osteo Assay Stripwell Plate[®] with M-CSF and RANKL in the presence or absence of curdlan. Curdlan inhibited the stimulatory effect of M-CSF and RANKL on bone resorption in a dose-dependent manner up to 50 μ g/ml (Fig. 1C and 1D). The actin sealing ring in osteoclasts is essential for bone resorption. We therefore visualized the actin cytoskeleton of

differentiated BMCs by rhodamine-phalloidin staining. As shown in Fig. 1E, M-CSF and RANKL treatment induced well-defined actin sealing ring formation, with a higher intensity ring height at the cell margin. Conversely, curdlan significantly decreased the number of well-defined actin rings and reduced their intensity. Curdlan had no effect on the proliferation of BMCs (data not shown).

Curdlan-dectin-1 interaction inhibits osteoclast formation and function in RAW cells – Since the results from Figure 1 suggested the potential relevance of curdlan in the regulation of osteoclastogenesis, we analyzed the expression of the curdlan specific receptor, dectin-1 in osteoclast precursors and stromal cells. We confirmed the expression of dectin-1 in osteoclast precursor RAW 264.7 cells and BMCs (Fig. 2A and 2B). In contrast, dectin-1 gene expression was not observed in stromal ST2 cells, suggesting that the target cells of curdlan in the regulation of osteoclastogenesis are osteoclast precursors cells, not osteoblasts/stromal cells. These data was supported by the result that curdlan significantly suppressed osteoclast differentiation from osteoclast precursors derived from BMCs (Fig. 2C and 2D). Therefore, the inhibitory effect of curdlan on the osteoclastogenesis of RAW 264.7 cells was evaluated *in vitro*. We found curdlan had no effect on cell proliferation of c-RAWs and d-RAWs (data not shown). After 7 days incubation with curdlan (12.5 μ g/ml), there was a 58.8% decrease in the number of osteoclasts differentiated by RANKL in d-RAWs (Fig. 3A and 3B). This effect of curdlan was dose-dependent, with maximum inhibition observed at 100 μ g/ml (97.0 % inhibition). On the other hand, curdlan slightly suppressed osteoclast formation in c-RAWs, and significant inhibition was observed only at a dose of 100 μ g/ml. Curdlan also inhibited RANKL-induced bone resorption (Fig. 3C and 3D) and actin ring formation (Fig. 3E) in differentiated d-RAWs.

Curdlan has no effect on M-CSF-induced BMC differentiation, but inhibits RANKL-induced osteoclast formation at early stage – Osteoclastogenesis is a multi-step process that can be separated into two major events: (1) the proliferation of BMCs and their differentiation into osteoclast precursors, induced by M-CSF; and (2) the subsequent differentiation of osteoclast precursors into osteoclasts, induced by RANKL (29). To examine which is the most important step to induce the suppressive effect of curdlan on

osteoclastogenesis, we first investigated the effect of curdlan on BMC differentiation induced by M-CSF. Curdlan had almost no effect on M-CSF-induced osteoclast formation (Fig. 4A and 4B, d1-4). To examine the precise effects of curdlan on BMC differentiation into osteoclast precursors induced by M-CSF, the expression level of an M-CSF-induced osteoclast precursor marker RANK was assessed by western blotting. However, curdlan had little effect on the expression of RANK induced by M-CSF (data not shown).

To determine the effect of curdlan on RANKL-induced differentiation of osteoclast precursor cells into mature osteoclasts, we examined the differentiation process of BMCs during 8-day RANKL stimulation in the presence or absence of curdlan. We observed that stimulation of curdlan strongly inhibited RANKL-induced osteoclast differentiation during the early stage (d4-6) of differentiation. However, curdlan had no inhibitory effect on osteoclast differentiation at later stages (d6-8). In d-RAWs, treatment with curdlan during the early stage (d1-3) had an almost identical suppressive effect on osteoclast differentiation induced by RANKL (Fig. 4C and 4D).

Curdlan has little effect on mature osteoclast bone resorption and actin ring formation – We investigated whether curdlan inhibited osteoclast bone resorption. When BMCs were cultured on dentin slices, mature osteoclasts caused the resorption of lacunae and the formation of pits in the presence of M-CSF and RANKL. The number and area of pits on the surface of the dentin slices were markedly decreased by the addition of curdlan at the beginning of the assay (Fig. 5A and 5B). However, after M-CSF and RANKL stimulation for 6 days on RedCell[®] (CellSeed Inc., Tokyo, Japan), mature osteoclasts formed and were then seeded on dentin slices, followed by incubation in the presence or absence of curdlan for an additional 2 days. Bone resorption pits and erosion areas showed no significant differences between the control slices and curdlan-treated slices (Fig. 5C and 5D). To investigate the effect of curdlan on mature osteoclasts, we examined actin ring formation. Curdlan exerted little effect on the actin ring formation of mature osteoclast (Fig. 5E).

Curdlan inhibits RANKL mediated NFATc1 expression via dectin-1 – NFATc1 is a transcription factor essential for RANKL-stimulated osteoclastogenesis (30).

Therefore, we investigated *Nfatc1* mRNA accumulation, which is related to the autoamplification of NFATc1. After 72 h of incubation with RANKL, there was a strong increase of *Nfatc1* mRNA copy number, compared to untreated cells. Culturing with curdlan suppressed stimulation of *Nfatc1* mRNA expression by RANKL in d-RAWs (Fig. 6A). In contrast, curdlan had almost no effect on expression levels of *Nfatc1* mRNA stimulated by RANKL in c-RAWs. As shown in Fig. 6B, the level of NFATc1 protein expression was increased in d-RAWs 72 h after stimulation with RANKL, and that stimulation was down-regulated by addition of curdlan. Similar results were obtained for M-CSF and RANKL-induced NFATc1 protein expression in BMCs (Fig. 6C).

Curdlan negatively regulates expression of osteoclastogenic genes – To substantiate further the effect of curdlan on osteoclastogenesis, we examined expression levels of mRNAs encoding osteoclast-related genes after 72 h of RANKL stimulation in d-RAWs. Consistent with the finding for osteoclastogenesis, the expression profiles revealed that osteoclast-associated genes, including *Trap* (Fig. 7A), *Oc-stamp* (Fig. 7B), *Cathepsin K* (Fig. 7C) and *Mmp9* (Fig. 7D), induced by RANKL, were significantly decreased by curdlan.

Curdlan inhibits the RANKL mediated AP-1 signaling pathway via dectin-1 – To investigate the molecular mechanism by which curdlan inhibits osteoclastogenesis, we evaluated the effect of curdlan on the activation of NF- κ B and AP-1, which is required for induction of NFATc1, by western blotting. RANKL induced NF- κ B activation, which was observed by I κ B- α degradation (Fig. 8A). Furthermore, the levels of c-jun phosphorylation (phospho-c-jun, Fig. 8B) and c-fos (Fig. 8C) expression were elevated by RANKL. When d-RAWs were incubated with RANKL and curdlan, the level of c-fos expression was lower than in cells treated with RANKL alone. This inhibitory effect of curdlan on RANKL-induced c-fos expression was not significant in c-RAWs. On the other hand, the activation of c-jun or I κ B- α protein induced by RANKL was not affected by treatment with curdlan.

Curdlan inhibits NFATc1 translocation to the nucleus – NFATc1, which is phosphorylated in the cell cytoplasm, is translocated from the cytoplasm to the nucleus by calcineurin-mediated dephosphorylation. We therefore investigated

whether RANKL-induced NFATc1 translocation is suppressed by curdlan treatment. Nuclear translocation of NFATc1 was detected in d-RAWs treated with RANKL and was observed to be down-regulated by addition of curdlan. (Fig. 9A and 9B). Western blotting analysis revealed that NFATc1 in the nuclear fraction was increased in cells following stimulation with RANKL. When cells were incubated with both RANKL and curdlan, the level of NFATc1 protein in the nucleus was lower than in cells treated with RANKL alone (Fig. 9C).

Curdlan inhibits osteoclastogenesis via degradation of Syk protein – To clarify the role of Syk on osteoclastogenesis, we examined Syk expression in d-RAWs incubated with curdlan by immunoblot analysis. Surprisingly, time-dependent Syk degradation was observed in the presence of curdlan up to 3 h, whereas curdlan transiently phosphorylated Syk protein in d-RAWs from 15 to 60 min (Fig. 10A). By immunofluorescence analysis, d-RAWs at all examined culture times exhibited a background level of Syk that was primarily localized in the cytoplasm. Syk protein accumulation was also diminished by curdlan treatment up to 3 h (Figure 10B). To confirm involvement of Syk in osteoclast formation, d-RAWs were transfected with Syk siRNA and cultured with RANKL. Using Syk-specific siRNA transfected into d-RAWs, Syk mRNA was knocked down by ~50% compared with cells transfected with a non-specific control siRNA (Fig. 10C). The knockdown of Syk protein was also confirmed by western blot analysis (Fig. 10D). In d-RAWs transfected with control siRNA, RANKL-induced osteoclast formation was observed. However, in the Syk-specific siRNA-treated d-RAWs, osteoclast formation was diminished even with RANKL treatment (Fig. 10E and 10F). Furthermore, the RANKL-induced increase in NFATc1 expression was blocked in the presence of Syk siRNA (Fig. 10G).

Inhibition of Syk activation abolished RANKL-induced osteoclastogenesis – To substantiate further the role of curdlan-dectin-1-Syk signaling in osteoclast formation, induced by RANKL, d-RAWs were pre-treated with the specific inhibitor for Syk. Two reagents, piceatannol and BAY 61-3606, are commonly used to block phosphorylation of Syk (31, 32). WST-1 analysis revealed that these inhibitors had no effect on d-RAW cell growth (data not shown) in the presence or absence of

RANKL. Both piceatannol and BAY 61-3606 pre-treatments effectively blocked RANKL-induced osteoclast formation in a dose-dependent manner (Fig. 11A-D). Furthermore, the increase in NFATc1 expression, induced by RANKL, was decreased by pre-treatment with both inhibitors (Fig. 11E).

DISCUSSION

A number of studies have documented β -glucan modulation of biological activities in macrophages (11, 33, 34). Osteoclasts are large, multinucleated cells formed by the fusion of precursor cells in the monocyte/macrophage lineage (35). There is considerable overlap of molecules and regulatory mechanisms shared between osseous and immune systems. With the aid of modern conditional gene targeting and transgenic technologies, the field of combined bone and immunology, known as osteoimmunology, is rapidly advancing. Previous studies have reported the existence of a specific β -glucan receptor, dectin-1, on effector cells, including macrophages (36-38). This receptor binding process is thought to be the first step in mediating the activating immunomodulatory effects of β -glucans.

Osteoclasts are derived from myeloid progenitors, which also give rise to monocytes, macrophages and dendritic cells. The direct effects of β -glucan on osteoclastogenesis have never been investigated to date. In the present study, we used curdlan, a linear β -1, 3-glucan from the bacterium *Alcaligenes faecalis*, as dectin-1 specific agonist (39-42). Interestingly, osteoclast formation of BMCs, induced by M-CSF and RANKL, was decreased by addition of curdlan (Fig. 1A and 1B), indicating that curdlan has protective effects against osteoclastogenesis. This effect appears not to be due to the toxicity of curdlan, because curdlan treatment did not alter the proliferation of BMCs significantly compared with M-CSF and RANKL (data not shown).

Bone resorption is a multi-step process initiated by the proliferation of immature osteoclast precursors. This is followed by commitment of these cells to the osteoclast phenotype and degradation of the organic and inorganic phases of bone by mature resorptive cells. When cultured with bone or dentin, osteoclasts excavate resorptive lacunae or pits, which are similar to the structures formed when cells degrade bone *in vivo*. Furthermore, the size of the resorption lacunae formed *in vitro* is used as

a quantitative measure of osteoclast activity (43). In this study, we used an Osteo Assay Stripwell Plate[®] coated with calcium phosphate substrate and observed down-regulation of the pit-forming activity of osteoclasts stimulated with M-CSF and RANKL (Fig. 1C and 1D). In addition, actin cytoskeletal organization includes the ruffled membranes and the actin ring or sealing zone, which is essential for mature osteoclasts to perform bone resorption (27, 28, 44, 45). Curdlan treatment showed impaired actin cytoskeletal organization in BMCs, suggesting that curdlan is involved in the regulation of actin ring formation induced by M-CSF and RANKL (Fig. 1E).

The cell specificity of dectin-1 expression suggested that the antiosteoclastogenic effect of curdlan was mainly dependent on osteoclast precursors, not osteoblast/stromal cells (Fig. 2). Then, we used a homogeneous clonal population of murine monocyte RAW 264.7 cells to elucidate the direct effects of RANKL and curdlan on osteoclast differentiation and function. This cell line is known to express RANK and differentiate into TRAP-positive cells when cultured with bone slices and RANKL (46). The main advantage of this system is that it does not contain any osteoblast/bone marrow stromal cells, which may also be targets of RANKL and curdlan actions. We also found that, when induced by RANKL, curdlan suppressed osteoclast formation (Fig. 3A and 3B), bone resorption (Fig. 3C and 3D) and actin ring formation (Fig. 3E) in RAW 264.7 cells retrovirally transduced to over-express dectin-1 (d-RAWs), as well as BMCs. On the basis of these findings, we speculate that dectin-1 is a principal receptor responsible for the regulation of osteoclast formation and activation mediated by curdlan. In contrast to d-RAWs, c-RAWs showed less responsiveness to the inhibitory effect of curdlan on RANKL-induced osteoclast formation. These findings are consistent with reports showing RAW 264.7 cells express low levels of endogenous dectin-1, as measured by flow cytometry (10).

M-CSF and RANKL are essential and sufficient to promote osteoclastogenesis. M-CSF can induce proliferation of BMCs and their differentiation into osteoclast precursors, and RANKL can subsequently induce differentiation of osteoclast precursors into mature osteoclasts (29, 35). The present study revealed that curdlan had no effect on M-CSF-induced BMC proliferation and differentiation, whereas curdlan inhibited RANKL-induced differentiation of

osteoclast precursors into osteoclasts at early stages (Fig. 4). These data are also supported by the findings that curdlan had little effect on the expression of RANK protein induced by M-CSF (data not shown). We also demonstrated that curdlan had no effect on bone resorption activity and actin ring formation of mature osteoclasts (Fig. 5). Together, these results indicate that curdlan suppressed RANKL-induced osteoclastogenesis at the step of osteoclast precursor differentiation into mature osteoclasts, and suggests that curdlan modulated the RANKL signaling pathway.

Previous studies have demonstrated that NFATc1 is strongly induced by RANKL and is required for terminal differentiation of osteoclasts (30, 47). We found that the level of NFATc1 expression during osteoclastogenesis was decreased by curdlan in d-RAWs and BMCs. In contrast, we did not observe a change in RANKL-induced NFATc1 expression in c-RAWs treated with curdlan (Fig. 6). These results indicate that curdlan-dectin-1 interaction impairs RANKL-induced osteoclastogenesis via suppression of NFATc1.

The inhibitory effect of curdlan on osteoclastogenesis was also confirmed by evaluating RANKL-induced mRNA expression levels of osteoclast-related genes. TRAP (48), Cathepsin K (49) and MMP9 (50) are required for bone resorptive activity of mature osteoclast, whereas OC-STAMP is essential for cell-cell fusion of osteoclasts (51). Based on promoter analyses, TRAP (30, 52, 53), cathepsin K (52, 54) and MMP9 (55) are regulated by NFATc1. In addition, a study using a specific inhibitor of NFAT revealed that OC-STAMP expression also requires NFATc1 in osteoclasts (51). Our results show that curdlan markedly decreased osteoclast-related gene expression regulated by NFATc1 in d-RAWs (Fig. 7). It is possible that the curdlan-dectin-1 interaction changes the RANKL-NFATc1 axis, with an ultimate decrease in osteoclast development, in addition to decreased NFATc1 production.

We also examined the mechanism by which curdlan suppressed RANKL-mediated NFATc1 expression. NF- κ B is involved in the activation of immediate-early responsive genes to RANKL (56) and is important for the initial induction of NFATc1 (57). On the other hand, NFATc1 is activated and binds its own promoter. After the induction of NFATc1, the combination of AP-1 complex containing c-fos and the continuous activation of calcium signaling allows for the

sustained autoamplification of NFATc1 (57). Western blotting analysis revealed that curdlan inhibited RANKL-stimulated c-fos protein expression, but not activation of NF- κ B (Fig. 8). These findings led us to speculate that inhibition of RANKL-stimulated NFATc1 expression by curdlan in d-RAWs, may occur because of suppression of AP-1 signaling pathway, which regulates autoamplification of NFATc1. This speculation was strongly supported by the observation that curdlan interferes with RANKL-induced nuclear translocation of NFATc1 (Fig. 9). However, curdlan itself appears to increase phosphorylation of c-jun protein in d-RAWs but not c-RAWs and activation of c-fos by RANKL was lower in d-RAWs than c-RAWs, indicating an alternative signaling pathway in osteoclastogenesis by curdlan. We have no precise explanation for this phenomenon and further studies are required to identify the detailed regulatory mechanisms of dectin-1 on osteoclast formation. The molecular mechanisms of the interaction between curdlan and dectin-1 are currently under investigation using dectin-1 deficient mice.

Syk has been identified to be involved in dectin-1 signaling, which is activated by engagement with β -glucan (12, 21, 58). Interestingly, treatment with curdlan increased Syk protein degradation in d-RAWs (Fig. 10A and 10B), suggesting that suppression of dectin-1/Syk signaling by curdlan inhibits RANKL-induced osteoclastogenesis. However, real-time RT-PCR analysis revealed that curdlan treatment did not alter mRNA expression of Syk in d-RAWs (data not shown). On the other hand, the addition of curdlan significantly increased the level of phosphorylated Syk in d-RAWs. A previous study using B cells reported that subsequent to ITAM

binding, Syk was phosphorylated on tyrosine 323, which generated a binding site for ubiquitin ligase, resulting in Syk ubiquitination and down-regulation of downstream signaling (59). From these results, the molecular mechanism for post-translational modifications, including phosphorylation, ubiquitination, SUMOylation, acetylation and O-glycosylation, are currently under investigation in our laboratory.

The importance of the dectin-1-Syk interaction in osteoclastogenesis was clearly demonstrated by the dramatic decrease in osteoclast formation (Fig. 10E and 10F) and NFATc1 expression (Fig. 10G) induced by Syk knockdown. These findings are consistent with a previous study, which reported that osteoclasts from Syk^{-/-} precursors (obtained from bone marrow chimeras generated using Syk^{-/-} fetal liver cells) (60) failed to differentiate normally *in vitro* (24).

Syk is a tyrosine kinase and a key mediator of ITAM receptor signaling (61), which is an important regulatory mechanism in osteoclast differentiation and activity (25, 62). We also found chemical inhibitors of Syk, down-regulated osteoclast formation (Fig. 11A-11D) and NFATc1 expression (Fig. 11E) induced by RANKL. These results are consistent with the premise that curdlan is a potent negative regulator of Syk signaling in osteoclasts. Taken together, these findings obtained in this study suggest that curdlan-dectin-1 binding strongly inhibits NFATc1 expression during osteoclast formation through down-regulation of Syk signaling in osteoclast progenitor cells. Therefore, one might expect that the curdlan administration could be a potential candidate for the treatment of osteoclast-related diseases such as osteoporosis.

REFERENCES

1. Suda, T., Takahashi, N., and Martin, T.J. (1992) Modulation of osteoclast differentiation. *Endocr. Rev.* **13**, 66-80
2. Suda, T., Takahashi, N., Udagawa, N., Jimi, E., Gillespie, M.T., and Martin, T.J. (1999) Modulation of osteoclast differentiation and function by the new members of the tumor necrosis factor receptor and ligand families. *Endocr. Rev.* **20**, 345-357
3. Darnay, B.G., Haridas, V., Ni, J., Moore, P.A., and Aggarwal, B.B. (1998) Characterization of the intracellular domain of receptor activator of NF- κ B (RANK): interaction with tumor necrosis factor receptor-associated factors and activation of NF- κ B and c-Jun N-terminal kinase. *J. Biol. Chem.* **273**, 20551-20555
4. Asagiri, M., and Takayanagi, H. (2007) The molecular understanding of osteoclast differentiation. *Bone* **40**, 251-264
5. Janeway, C.A. Jr. (1989) Approaching the asymptote? Evolution and revolution in immunology. *Cold Spring Harb. Symp. Quant. Biol.* **54**, 1-13
6. Brown, G.D., Gordon, S. (2001) Immune recognition. A new receptor for beta-glucans. *Nature* **413**, 36-37
7. Ariizumi, K., Shen, G.L., Shikano, S., Xu, S., Ritter, R. III., Kumamoto, T., Edelbaum, D., Morita, A., Bergstresser, P.R., and Takashima, A. (2000) Identification of a novel, dendritic cell-associated molecule, dectin-1, by subtractive cDNA cloning. *J. Biol. Chem.* **275**, 20157-20167
8. Taylor, P.R., Brown, G.D., Reid, D.M., Willment, J.A., Martinez-Pomares, L., Gordon, S., and Wong, S.Y. (2002) The beta-glucan receptor, dectin-1, is predominantly expressed on the surface of cells of the monocyte/macrophage and neutrophil lineages. *J. Immunol.* **169**, 3876-3882
9. Brown, G.D., Taylor, P.R., Reid, D.M., Willment, J.A., Williams, D.L., Martinez-Pomares, L., Wong, S.Y., and Gordon, S. (2002) Dectin-1 is a major beta-glucan receptor on macrophages. *J. Exp. Med.* **196**, 407-412
10. Brown, G.D., Herre, J., Williams, D.L., Willment, J.A., Marshall, A.S., and Gordon, S. (2003) Dectin-1 mediates the biological effects of beta-glucans. *J. Exp. Med.* **197**, 1119-1124
11. Rogers, N.C., Slack, E.C., Edwards, A.D., Nolte, M.A., Schulz, O., Schweighoffer, E., Williams, D.L., Gordon, S., Tybulewicz, V.L., Brown, G.D., and Reis e Sousa, C. (2005) Syk-dependent cytokine induction by Dectin-1 reveals a novel pattern recognition pathway for C type lectins. *Immunity* **22**, 507-517
12. Underhill, D.M., Rossnagle, E., Lowell, C.A., and Simmons, R.M. (2005) Dectin-1 activates Syk tyrosine kinase in a dynamic subset of macrophages for reactive oxygen production. *Blood* **106**, 2543-2550
13. Drummond, R.A., Saijo, S., Iwakura, Y., and Brown, G.D. (2011) The role of Syk/CARD9 coupled C-type lectins in antifungal immunity. *Eur. J. Immunol.* **41**, 276-281
14. Osorio, F., and Reis e Sousa C. (2011) Myeloid C-type lectin receptors in pathogen recognition and host defense. *Immunity* **34**, 651-664
15. Brown, G.D., and Gordon, S. (2003) Fungal beta-glucans and mammalian immunity. *Immunity* **19**, 311-315
16. Czop, J.K. (1986) The role of beta-glucan receptors on blood and tissue leukocytes in phagocytosis and metabolic activation. *Pathol. Immunopathol. Res.* **5**, 286-296
17. Williams, D.L. (1997) Overview of (1 \rightarrow 3)-beta-D-glucan immunobiology. *Mediators Inflamm.* **6**, 247-250
18. Ross, G.D., Vetvicka, V., Yan, J., Xia, Y., and Vetvicková, J. (1999) Therapeutic intervention with complement and beta-glucan in cancer. *Immunopharmacology* **42**, 61-74
19. Williams, D.L., Mueller, A., and Browder, W. (1996) Glucan-based macrophage stimulators. *Clinical Immunotherapy* **5**, 392-399
20. Castro, G.R., Panilaitis, B., Bora, E., and Kaplan, D.L. (2007) Controlled release biopolymers for enhancing the immune response. *Mol. Pharm.* **4**, 33-46
21. Mocanu, G., Mihai, D., Moscovici, M., Picton, L., LeCerf, D. (2009) Curdian microspheres. Synthesis, characterization and interaction with proteins (enzymes, vaccines). *Int. J. Biol. Macromol.* **44**, 215-221

22. Koga, T., Inui, M., Inoue, K., Kim, S., Suematsu, A., Kobayashi, E., Iwata, T., Ohnishi, H., Matozaki, T., Kodama, T., Taniguchi, T., Takayanagi, H., and Takai, T. (2004) Costimulatory signals mediated by the ITAM motif cooperate with RANKL for bone homeostasis. *Nature* **428**, 758-63
23. Faccio, R., Zou, W., Colaianni, G., Teitelbaum, S.L., and Ross, F.P. (2003) High dose M-CSF partially rescues the *Dap12*^{-/-} osteoclast phenotype. *J. Cell Biochem.* **90**, 871-883
24. Mócsai, A., Humphrey, M.B., Van, Ziffle, J.A., Hu, Y., Burghardt, A., Spusta, S.C., Majumdar, S., Lanier, L.L., Lowell, C.A., and Nakamura, M.C. (2004) The immunomodulatory adapter proteins DAPI2 and Fc receptor gamma-chain (FcR γ) regulate development of functional osteoclasts through the Syk tyrosine kinase. *Proc. Natl. Acad. Sci. U. S. A.* **101**, 6158-6163
25. Zou, W., Kitaura, H., Reeve, J., Long, F., Tybulewicz, V.L., Shattil, S.J., Ginsberg, M.H., Ross, F.P., and Teitelbaum, S.L. (2007) Syk, c-Src, the α v β 3 integrin, and ITAM immunoreceptors, in concert, regulate osteoclastic bone resorption. *J. Cell. Biol.* **176**, 877-888
26. Saltel, F., Destaing, O., Bard, F., Eichert, D., and Jurdic, P. (2004) Apatite-mediated actin dynamics in resorbing osteoclasts. *Mol. Biol. Cell* **15**, 5231-5241
27. Boyce, B.F., Yoneda, T., Lowe, C., Soriano, P., and Mundy, G.R. (1992) Requirement of pp60c-src expression for osteoclasts to form ruffled borders and resorb bone in mice. *J. Clin. Invest.* **90**, 1622-1627
28. Teitelbaum, S.L., and Ross, F.P. (2003) Genetic regulation of osteoclast development and function. *Nat Rev Genet.* **4**, 638-649
29. Takahashi, N., Udagawa, N., Tanaka, S., and Suda, T. (2003) Generating murine osteoclasts from bone marrow. *Methods. Mol. Med.* **80**, 129-144
30. Takayanagi, H., Kim, S., Koga, T., Nishina, H., Isshiki, M., Yoshida, H., Saiura, A., Isobe, M., Yokochi, T., Inoue, J., Wagner, E.F., Mak, T.W., Kodama, T., and Taniguchi, T. (2002) Induction and activation of the transcription factor NFATc1 (NFAT2) integrate RANKL signaling in terminal differentiation of osteoclasts. *Dev Cell.* **3**, 889-901
31. Eiseman, E., and Bolen, J.B. (1992) Engagement of the high-affinity IgE receptor activates src protein-related tyrosine kinases. *Nature* **355**, 78-80
32. Yamamoto, N., Takeshita, K., Shichijo, M., Kokubo, T., Sato, M., Nakashima, K., Ishimori, M., Nagai, H., Li, Y.F., Yura, T., and Bacon, K.B. (2003) The orally available spleen tyrosine kinase inhibitor 2-[7-(3,4-dimethoxyphenyl)-imidazo[1,2-c]pyrimidin-5-ylamino] nicotinamide dihydrochloride (BAY 61-3606) blocks antigen-induced airway inflammation in rodents. *J. Pharmacol. Exp. Ther.* **306**, 1174-1181
33. Adachi, Y., Ishii, T., Ikeda, Y., Hoshino, A., Tamura, H., Aketagawa, J., Tanaka, S., and Ohno, N. (2004) Characterization of beta-glucan recognition site on C-type lectin, dectin-1. *Infect. Immun.* **72**, 4159-4171
34. Chaung, H.C., Huang, T.C., Yu, J.H., Wu, M.L., Chung, W.B. (2009) Immunomodulatory effects of beta-glucans on porcine alveolar macrophages and bone marrow haematopoietic cell-derived dendritic cells. *Vet. Immunol. Immunopathol.* **131**, 147-157
35. Takayanagi, H. (2007) Osteoimmunology: shared mechanisms and crosstalk between the immune and bone systems. *Nat. Rev. Immunol.* **7**, 292-304
36. Brown, G.D. (2006) Dectin-1: a signalling non-TLR pattern-recognition receptor. *Nat. Rev. Immunol.* **6**, 33-43
37. Willment, J.A., Gordon, S., and Brown, G.D. Characterization of the human beta-glucan receptor and its alternatively spliced isoforms. *J. Biol. Chem.* **276**, 43818-43823
38. Kerrigan, A.M., Brown, G.D. (2009) C-type lectins and phagocytosis. *Immunobiology* **214**, 562-575
39. Kataoka, K., Muta, T., Yamazaki, S., and Takeshige K. (2002) Activation of macrophages by linear (1right-arrow3)-beta-D-glucans. Implications for the recognition of fungi by innate immunity. *J. Biol. Chem.* **277**, 36825-36831
40. Gantner, B.N., Simmons, R.M., Canavera, S.J., Akira, S., and Underhill, D.M. (2003) Collaborative induction of inflammatory responses by dectin-1 and Toll-like receptor 2. *J. Exp. Med.* **197**, 1107-1117
41. Palma, A.S., Feizi, T., Zhang, Y., Stoll, M.S., Lawson, A.M., Díaz-Rodríguez, E.,

- Campanero-Rhodes, M.A., Costa, J., Gordon, S., Brown, G.D., and Chai, W. (2006) Ligands for the beta-glucan receptor, Dectin-1, assigned using "designer" microarrays of oligosaccharide probes (neoglycolipids) generated from glucan polysaccharides. *J. Biol. Chem.* **281**, 5771-5779
42. Morita, A., Kirino, T., Hashi, K., Aoki, N., Fukuhara, S., Hashimoto, N., Nakayama, T., Sakai, M., Teramoto, A., Tominari, S., and Yoshimoto, T. (2012) The natural course of unruptured cerebral aneurysms in a Japanese cohort. *N. Engl. J. Med.* **366**, 2474-2482
43. Fuller, K., Thong, J.T., Breton, B.C., and Chambers, T.J. (1994) Automated three-dimensional characterization of osteoclastic resorption lacunae by stereoscopic scanning electron microscopy. *J. Bone Miner. Res.* **9**, 17-23
44. Teti, A., Marchisio, P.C., and Zallone, A.Z. (1991) Clear zone in osteoclast function: role of podosomes in regulation of bone-resorbing activity. *Am. J. Physiol.* **261**, C1-C7
45. Zou, W., and Teitelbaum, S.L. (2010) Integrins, growth factors, and the osteoclast cytoskeleton. *Ann. N. Y. Acad. Sci.* **1192**, 27-31
46. Hsu, H., Lacey, D.L., Dunstan, C.R., Solovyev, I., Colombero, A., Timms, E., Tan, H.L., Elliott, G., Kelley, M.J., Sarosi, I., Wang, L., Xia, X.Z., Elliott, R., Chiu, L., Black, T., Scully, S., Capparelli, C., Morony, S., Shimamoto, G., Bass, M.B., and Boyle, W.J. (1999) Tumor necrosis factor receptor family member RANK mediates osteoclast differentiation and activation induced by osteoprotegerin ligand. *Proc. Natl. Acad. Sci. U. S. A.* **96**, 3540-3545
47. Ishida, N., Hayashi, K., Hoshijima, M., Ogawa, T., Koga, S., Miyatake, Y., Kumegawa, M., Kimura, T., and Takeya, T. (2002) Large scale gene expression analysis of osteoclastogenesis in vitro and elucidation of NFAT2 as a key regulator. *J. Biol. Chem.* **277**, 41147-41156
48. Halleen, J.M., Räsänen, S., Salo, J.J., Reddy, S.V., Roodman, G.D., Hentunen, T.A., Lehenkari, P.P., Kaija, H., Vihko, P., and Väänänen, H.K. (1999) Intracellular fragmentation of bone resorption products by reactive oxygen species generated by osteoclastic tartrate-resistant acid phosphatase. *J. Biol. Chem.* **274**, 22907-22910
49. Ishikawa, T., Kamiyama, M., Tani-Ishii, N., Suzuki, H., Ichikawa, Y., Hamaguchi, Y., Momiyama, N., and Shimada, H. (2001) Inhibition of osteoclast differentiation and bone resorption by cathepsin K antisense oligonucleotides. *Mol. Carcinog.* **32**, 84-91
50. Ishibashi, O., Niwa, S., Kadoyama, K., and Inui, T. (2006) MMP-9 antisense oligodeoxynucleotide exerts an inhibitory effect on osteoclastic bone resorption by suppressing cell migration. *Life Sci.* **79**, 1657-1660
51. Miyamoto, H., Suzuki, T., Miyauchi, Y., Iwasaki, R., Kobayashi, T., Sato, Y., Miyamoto, K., Hoshi, H., Hashimoto, K., Yoshida, S., Hao, W., Mori, T., Kanagawa, H., Katsuyama, E., Fujie, A., Morioka, H., Matsumoto, M., Chiba, K., Takeya, M., Toyama, Y., and Miyamoto, T. (2012) Osteoclast stimulatory transmembrane protein and dendritic cell-specific transmembrane protein cooperatively modulate cell-cell fusion to form osteoclasts and foreign body giant cells. *J. Bone Miner. Res.* **27**, 1289-1297
52. Kim, Y., Sato, K., Asagiri, M., Morita, I., Soma, K., and Takayanagi, H. (2005) Contribution of nuclear factor of activated T cells c1 to the transcriptional control of immunoreceptor osteoclast-associated receptor but not triggering receptor expressed by myeloid cells-2 during osteoclastogenesis. *J. Biol. Chem.* **280**, 32905-32913
53. Matsuo, K., Galson, D.L., Zhao, C., Peng, L., Laplace, C., Wang, K.Z., Bachler, M.A., Amano, H., Aburatani, H., Ishikawa, H., and Wagner, E.F. (2004) Nuclear factor of activated T-cells (NFAT) rescues osteoclastogenesis in precursors lacking c-Fos. *J. Biol. Chem.* **279**, 26475-26480
54. Matsumoto, M., Kogawa, M., Wada, S., Takayanagi, H., Tsujimoto, M., Katayama, S., Hisatake, K., Nogi, Y. (2004) Essential role of p38 mitogen-activated protein kinase in cathepsin K gene expression during osteoclastogenesis through association of NFATc1 and PU.1. *J. Biol. Chem.* **279**, 45969-45979
55. Song, I., Kim, J.H., Kim, K., Jin, H.M., Youn, B.U., Kim, N. (2009) Regulatory mechanism of NFATc1 in RANKL-induced osteoclast activation. *FEBS Lett.* **583**, 2435-2440
56. Takatsuna, H., Asagiri, M., Kubota, T., Oka, K., Osada, T., Sugiyama, C., Saito, H., Aoki, K., Ohya, K., Takayanagi, H., and Umezawa K. (2005) Inhibition of RANKL-induced osteoclastogenesis by (-)-DHMEQ, a novel NF-kappaB inhibitor, through downregulation of NFATc1. *J. Bone Miner. Res.* **20**, 653-662

57. Asagiri, M., Sato, K., Usami, T., Ochi, S., Nishina, H., Yoshida, H., Morita, I., Wagner, E.F., Mak, T.W., Serfling, E., and Takayanagi, H. (2005) Autoamplification of NFATc1 expression determines its essential role in bone homeostasis. *J. Exp. Med.* **202**, 1261-1269
58. Gross, O., Gewies, A., Finger, K., Schäfer, M., Sparwasser, T., Peschel, C., Förster, I., and Ruland, J. (2006) Card9 controls a non-TLR signalling pathway for innate anti-fungal immunity. *Nature* **442**, 651-656
59. Rao, N., Dodge, I., and Band, H. (2002) The Cbl family of ubiquitin ligases. Critical negative regulators of tyrosine kinase signaling in the immune system. *J. Leukoc. Biol.* **71**, 753-763
60. Mócsai, A., Zhou, M., Meng, F., Tybulewicz, V.L., and Lowell, C.A. (2002) Syk is required for integrin signaling in neutrophils. *Immunity* **16**, 547-58
61. Humphrey, M.B., Lanier, L.L., and Nakamura, M.C. (2005) Role of ITAM-containing adapter proteins and their receptors in the immune system and bone. *Immunol. Rev.* **208**, 50-65
62. Solski, P.A., Wilder, R.S., Rossman, K.L., Sondek, J., Cox, A.D., Campbell, S.L., and Der, C.J. (2004) Requirement for C-terminal sequences in regulation of Ect2 guanine nucleotide exchange specificity and transformation. *J. Biol. Chem.* **279**, 25226-25233

FIGURE LEGENDS

FIGURE 1. Effect of curdlan on osteoclastogenesis in BMCs (A) Mouse BMCs were incubated with M-CSF (20 ng/ml) and RANKL (40 ng/ml) in the presence or absence of curdlan (12.5–50 µg/ml). Cells were cultured for 4 days and stained for TRAP activity. Bars indicate 500 µm. (B) The number of osteoclasts was counted after staining for TRAP activity. Data show the number of osteoclasts from 3 independent samples, and bars represent means ± standard deviation. Data were analyzed by Dunnett's test after one-way ANOVA ($***P < 0.0001$ in comparison to control without curdlan treatment). (C) BMCs were incubated with M-CSF (20 ng/ml) and RANKL (40 ng/ml) in the presence or absence of curdlan (12.5–50 µg/ml) on an Osteo Assay Stripwell Plate® for 7 days. Cells were removed and the resorption pits were visualized with light microscopy. Bars indicate 500 µm. (D) The pit areas were analyzed with ImageJ software. Data show the resorption area from 3 independent samples, and bars represent means ± standard deviation. Data were analyzed by Dunnett's test after one-way ANOVA ($*P < 0.05$ and $**P < 0.01$ in comparison to control without curdlan treatment). (E) BMCs were incubated with M-CSF (20 ng/ml) and RANKL (40 ng/ml) in the presence or absence of curdlan (12.5–50 µg/ml) for 5 days. Cells were fixed and stained for F-actin. Bars indicate 500 µm.

FIGURE 2. Expression of dectin-1 in c-RAWs, d-RAWs, BMCs and ST2 cells (A) Total RNA was isolated from c-RAWs, d-RAWs, BMCs and ST2, reverse transcribed into cDNA, then PCR amplification was performed using primers specific for *dectin-1* and *Gapdh*. Data show the fold changes in *dectin-1* mRNA copy number values from 3 independent samples and bars represent means ± standard deviation. (B) Whole cell lysates from c-RAW, d-RAW and BMCs were subjected to SDS-PAGE and western blotting analyses, with the blots probed for dectin-1. Equivalent protein aliquots of cell lysates were also analyzed for β-actin. (C) Mouse BMCs were incubated overnight on culture dishes in α-MEM containing 10% FCS. After discarding adherent cells, floating cells were further incubated with M-CSF (20 ng/ml) on Petri dishes, BMCs became adherent after a 3-day culture and were used as osteoclast precursors. Osteoclast precursors were further cultured with M-CSF + RANKL (40 ng/ml) in the presence or absence of curdlan (25 µg/ml) for 3 days. Cells were stained for TRAP activity. Bars indicate 500 µm. (D) The number of osteoclasts was counted after staining for TRAP activity. Data show the number of osteoclasts from 3 independent samples, and bars represent means ± standard deviation. Data were analyzed by Dunnett's test after one-way ANOVA ($***P < 0.0001$ in comparison to control without curdlan treatment).

FIGURE 3. Effect of curdlan on osteoclastogenesis in RAW 264.7 cells (A) c-RAWs and d-RAWs were incubated with RANKL (40 ng/ml) in the presence or absence of curdlan (12.5–50 µg/ml). Cells were cultured for 7 days and stained for TRAP activity. Bars indicate 500 µm. (B) The number of osteoclasts was counted after staining for TRAP activity. Data show the number of osteoclasts from 3 independent samples, and bars represent means ± standard deviation. Data were analyzed by Dunnett's test after one-way ANOVA ($**P < 0.01$ and $***P < 0.0001$ in comparison to control without curdlan treatment). (C) d-RAWs were incubated with RANKL (40 ng/ml) in the presence or absence of curdlan (25 µg/ml) on an Osteo Assay Stripwell Plate® for 12 days. Cells were removed and the resorption pits were visualized with light microscopy. Bars indicate 500 µm. (D) The pit areas were analyzed with ImageJ software. Data show the resorption area from 3 independent samples, and bars represent means ± standard deviation. Data were analyzed by Student *t* test ($**P < 0.01$ in comparison to control without curdlan treatment). (E) d-RAWs were incubated with RANKL (40 ng/ml) in the presence or absence of curdlan (25 µg/ml) for 8 days. Cells were fixed and stained for F-actin. Bars indicate 500 µm.

FIGURE 4. Time course effect of curdlan on osteoclast formation in BMCs and d-RAWs (A) BMCs were incubated with M-CSF (20 ng/ml) for 3 days and further cultured with M-CSF + RANKL (40 ng/ml) in the presence or absence of curdlan (25 µg/ml) for 4 days. Cells were stained for TRAP activity. Bars indicate 500 µm. (C) d-RAWs were incubated RANKL (40 ng/ml) in the presence or absence of curdlan (25 µg/ml). Cells were cultured for 7 days and stained for TRAP activity. Bars indicate 500 µm. The number of osteoclasts differentiated from BMCs (B) and d-RAWs (D) was counted after the staining for TRAP activity. Data show the number of osteoclasts from 3 independent samples, and bars represent

means \pm standard deviation. Data were analyzed by Dunnett's test after one-way ANOVA ($***P < 0.0001$ in comparison to control without curdlan treatment).

FIGURE 5. Time course effect of curdlan on osteoclast activity in BMCs (A) BMCs were incubated with M-CSF (20 ng/ml) and RANKL (40 ng/ml) in the presence or absence of curdlan (25 μ g/ml) on dentin slices for 7 days. Dentin slices were stained with Mayer's hematoxylin after removal of cells. The resorption pits were visualized by light microscopy. Bars indicate 200 μ m. (B) The pit areas were analyzed with ImageJ software. Data show the resorption area from 3 independent samples, and bars represent means \pm standard deviation. Data were analyzed by Dunnett's test after one-way ANOVA ($***P < 0.001$ compared with controls without curdlan treatment). (C) BMCs were incubated with M-CSF (20 ng/ml) and RANKL (40 ng/ml) using RedCell[®] for 5 days. Mature osteoclasts were harvested and seeded on dentin slices followed by treatment with or without curdlan (25 μ g/ml) for an additional 2 days. Dentin slices were stained with Mayer's hematoxylin after removal of cells. The resorption pits were visualized by light microscopy. Bars indicate 200 μ m. (D) The pit areas were analyzed with ImageJ software. Data show the resorption area from 3 independent samples, and bars represent means \pm standard deviation. (E) Mature osteoclasts were stimulated by curdlan (25 μ g/ml) for 1 day. Cells were fixed and stained for F-actin. Bars indicate 500 μ m.

FIGURE 6. Effect of curdlan on NFATc1 expression in RAW cells c-RAWs and d-RAWs were incubated with or without curdlan (25 μ g/ml) in the presence of RANKL (40 ng/ml) for 72 h. (A) Total RNA was isolated, reverse transcribed into cDNA, then PCR amplification was performed using primers specific for *Nfatc1* and *Gapdh*. Data show the fold changes in *Nfatc1* mRNA copy number values from 3 independent samples, and bars represent means \pm standard deviation. Data were analyzed by Tukey's post test after one-way ANOVA ($***P < 0.0001$ in comparison to treatment with RANKL). (B) Whole cell lysates were subjected to SDS-PAGE and western blotting analyses, with the blots probed for NFATc1. Equivalent protein aliquots of cell lysates were also analyzed for β -actin. (C) BMCs were incubated with or without curdlan (25 μ g/ml) in the presence or absence of M-CSF (20 ng/ml) and RANKL (40 ng/ml) for 48 h. Whole cell lysates were subjected to SDS-PAGE and western blotting analyses, with the blots probed for NFATc1. Equivalent protein aliquots of cell lysates were also analyzed for β -actin.

FIGURE 7. Effect of curdlan on RANKL-induced expression of osteoclastogenic genes in d-RAWs d-RAWs were incubated with or without curdlan (25 μ g/ml) in the presence of RANKL (40 ng/ml) for 72 h. Total RNA was isolated, reverse transcribed into cDNA, then PCR amplification was performed using primers specific for *Trap*, *Oc-stamp*, *Cathepsin K*, *Mmp9* and *Gapdh*. Data show the fold changes in *Trap* (A), *Oc-stamp* (B), *Cathepsin K* (C), and *Mmp9* (D) mRNA copy number values from 3 independent samples, and bars represent means \pm standard deviation. Data were analyzed by Tukey's post test after one-way ANOVA ($**P < 0.01$ and $***P < 0.0001$ in comparison to treatment with RANKL).

FIGURE 8. Effect of curdlan on RANKL-induced activation of osteoclast differentiation-related molecules in RAW cells c-RAWs and d-RAWs were incubated with or without curdlan (25 μ g/ml) in the presence of RANKL (40 ng/ml) for indicated time. Whole cell lysates were subjected to SDS-PAGE and western blotting analyses, with the blots probed for I κ B- α (A), phosphorylated c-jun (phospho-c-jun), c-jun (B) and c-fos (C). Equivalent protein aliquots of cell lysates were also analyzed for β -actin.

FIGURE 9. Effect of curdlan on RANKL-stimulated NFATc1 activity d-RAWs d-RAWs were incubated with or without curdlan (25 μ g/ml) in the presence of RANKL (40 ng/ml) for 3 h. (A) Cells were fixed, permeabilized and stained for NFATc1 (green) and nucleus (blue). Bars indicate 50 μ m. (B) Cells showing nuclear translocation of NFATc1 protein were scored. Data show the percentage of nuclear NFATc1 positive cells from 3 independent samples, and bars represent means \pm standard deviation. Data were analyzed by Student *t* test. The asterisk indicates $P < 0.05$ in comparison to treatment with RANKL. (C) d-RAWs (2×10^6 cells) were incubated with or without curdlan (25 μ g/ml) in the presence of RANKL (40 ng/ml) for 6 h. Whole cell lysates or nuclear fractions were prepared and analyzed by western blotting, with the blots probed for NFATc1. Equal sample loading and purity of nuclear fractions were controlled by analyzing β -actin and Histone H3.

FIGURE 10. Effect of silencing Syk on RANKL-induced osteoclastogenesis in d-RAWs d-RAWs were incubated with or without curdlan (25 $\mu\text{g/ml}$) for indicated time. (A) Whole cell lysates were subjected to SDS-PAGE and western blotting analyses, with the blots probed for Syk and phosphorylated Syk. Equivalent protein aliquots of cell lysates were also analyzed for β -actin. (B) Cells were fixed, permeabilized and stained for Syk (green) and nucleus (blue). Bars indicate 100 μm . d-RAWs were transfected as labeled in panels (C)–(G) with either control or Syk-specific siRNAs. (C) Total RNA was isolated from the transfected cells, reverse transcribed into cDNA, then PCR amplification was performed using primers specific for Syk and Gapdh. Data show the fold changes in Syk mRNA copy number values from 3 independent samples, and bars represent means \pm standard deviation. After transfection, cells were incubated in the presence of RANKL (40 ng/ml) for 7 days. (D) Whole cell lysates were isolated from the transfected cells, subjected to SDS-PAGE and western blotting analyses, with the blots probed for Syk. Equivalent protein aliquots of cell lysates were also analyzed for β -actin. (E) Cells were stained for TRAP activity. Bars indicate 500 μm . (F) The number of osteoclasts differentiated from transfected d-RAWs was counted after staining for TRAP activity. Data show the number of osteoclasts from 3 independent samples, and bars represent means \pm standard deviation. Data were analyzed by Dunnett's test after one-way ANOVA (** $P < 0.01$ in comparison to d-RAWs transfected control siRNA). (G) Transfected d-RAWs were incubated in the presence or absence of RANKL (40 ng/ml) for 72 h. Whole cell lysates were subjected to SDS-PAGE and western blotting analyses, with the blots probed for NFATc1. Equivalent protein aliquots of cell lysates were also analyzed for β -actin.

FIGURE 11. Effect of selective inhibitor for Syk on RANKL-induced osteoclastogenesis in d-RAWs d-RAWs were pre-treated with 5–20 μM of piceatannol (A) or 100–1000 nM of BAY 61-3606 (B) for 1 h. Cells were then incubated in the presence of RANKL (40 ng/ml) for 7 days. Cells were stained for TRAP activity. Bars indicate 500 μm . The number of osteoclasts differentiated from piceatannol- (C) and BAY 61-3606- (D) pre-treated cells were counted after staining for TRAP activity. Data show the number of osteoclasts from 3 independent samples, and bars represent means \pm standard deviation. Data were analyzed by Dunnett's test after one-way ANOVA (** $P < 0.01$ and *** $P < 0.0001$ in comparison to control without inhibitor pre-treatment). (E) d-RAWs were pre-treated with piceatannol (5–20 μM) or BAY 61-3606 (100–1000 nM) for 1 h. Cells were the incubated in the presence or absence of RANKL (40 ng/ml) for 72 h. Whole cell lysates were subjected to SDS-PAGE and western blotting analyses, with the blots probed for NFATc1. Equivalent protein aliquots of cell lysates were also analyzed for β -actin.

Figure 1

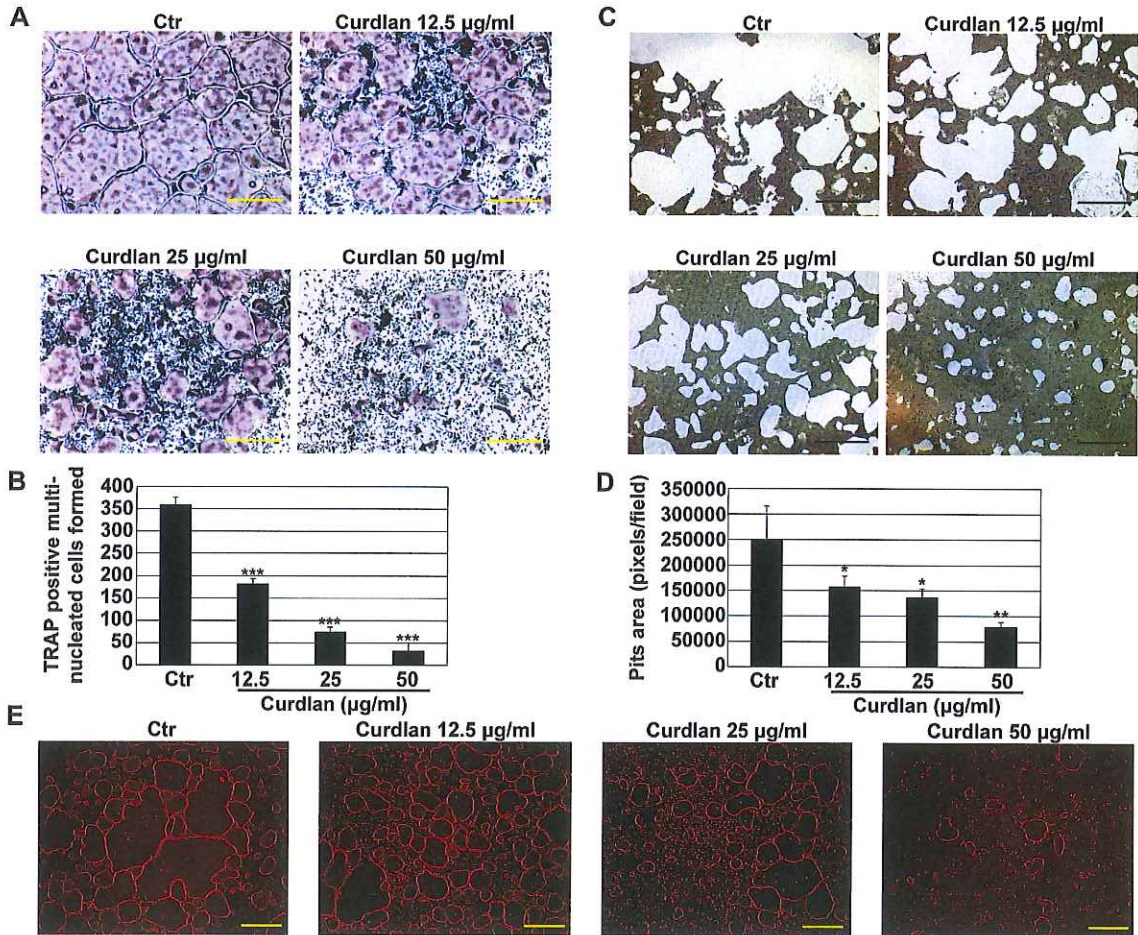


Figure 2

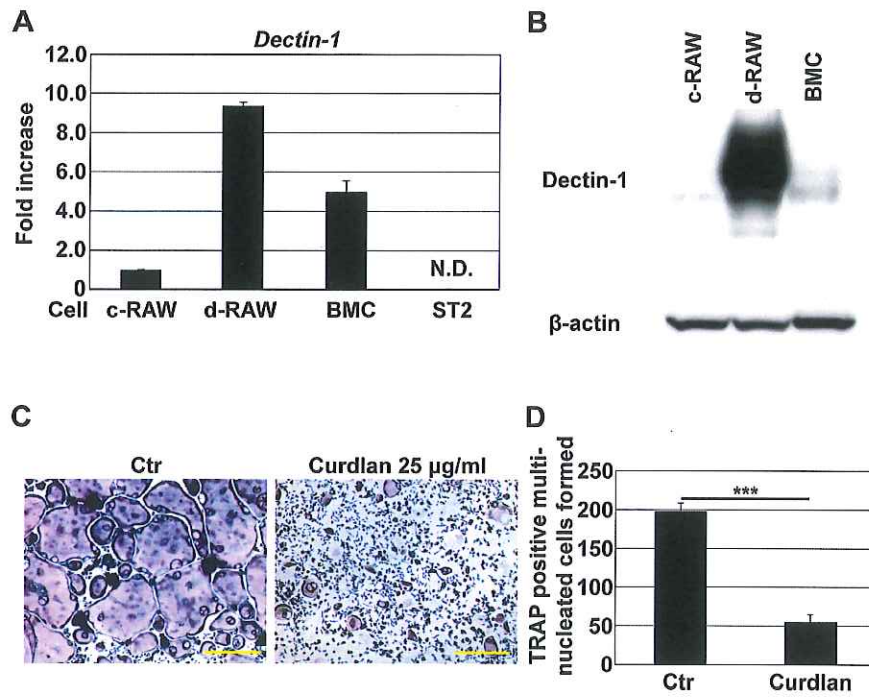


Figure 3

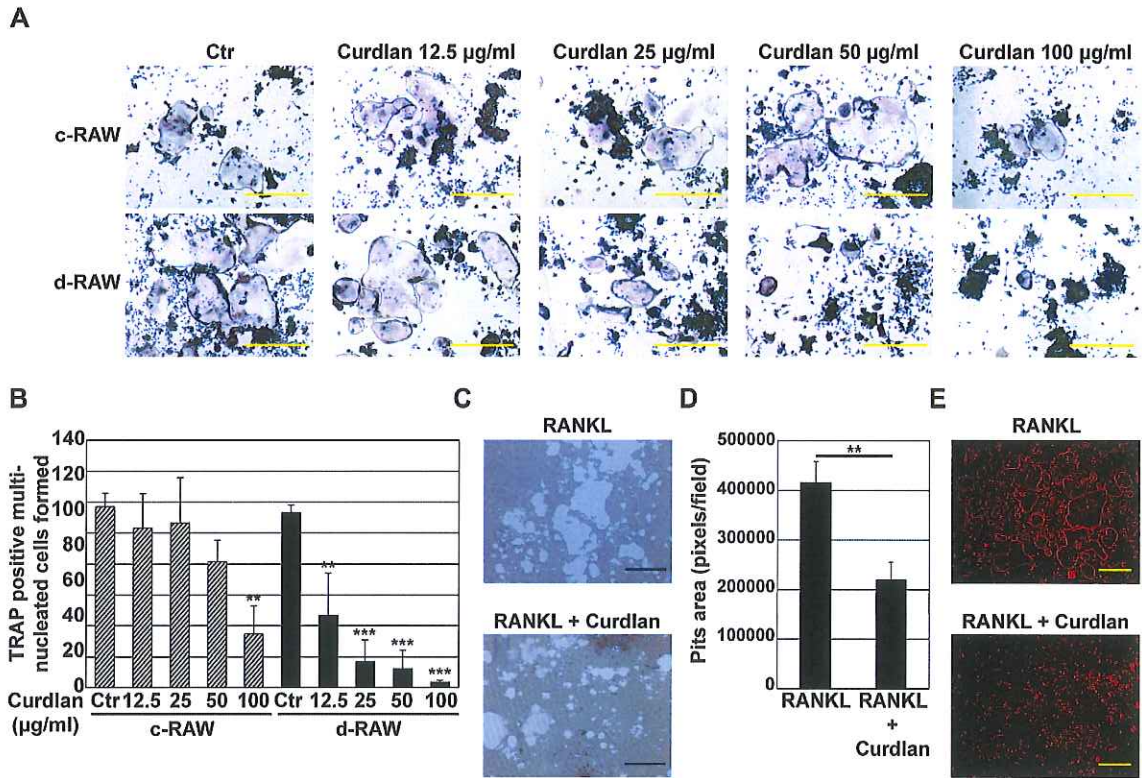


Figure 4

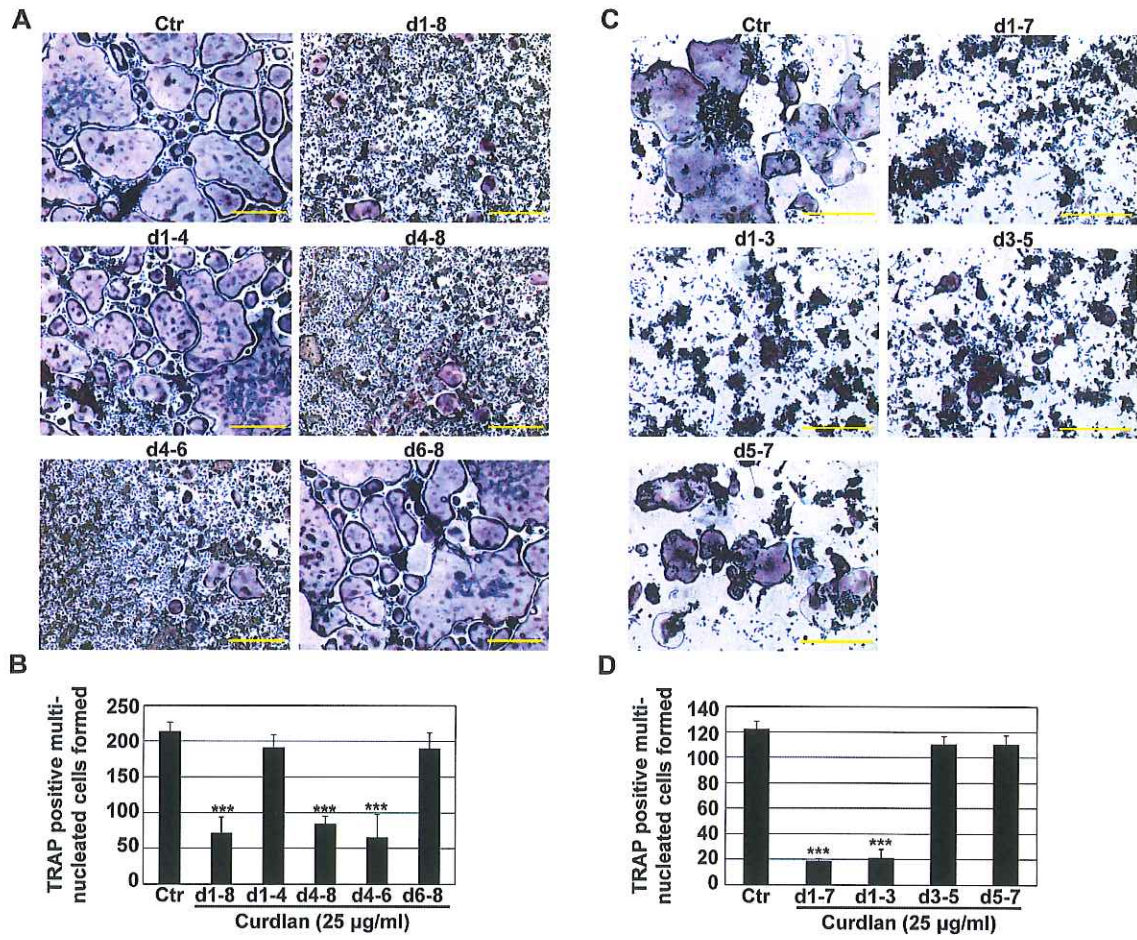


Figure 5

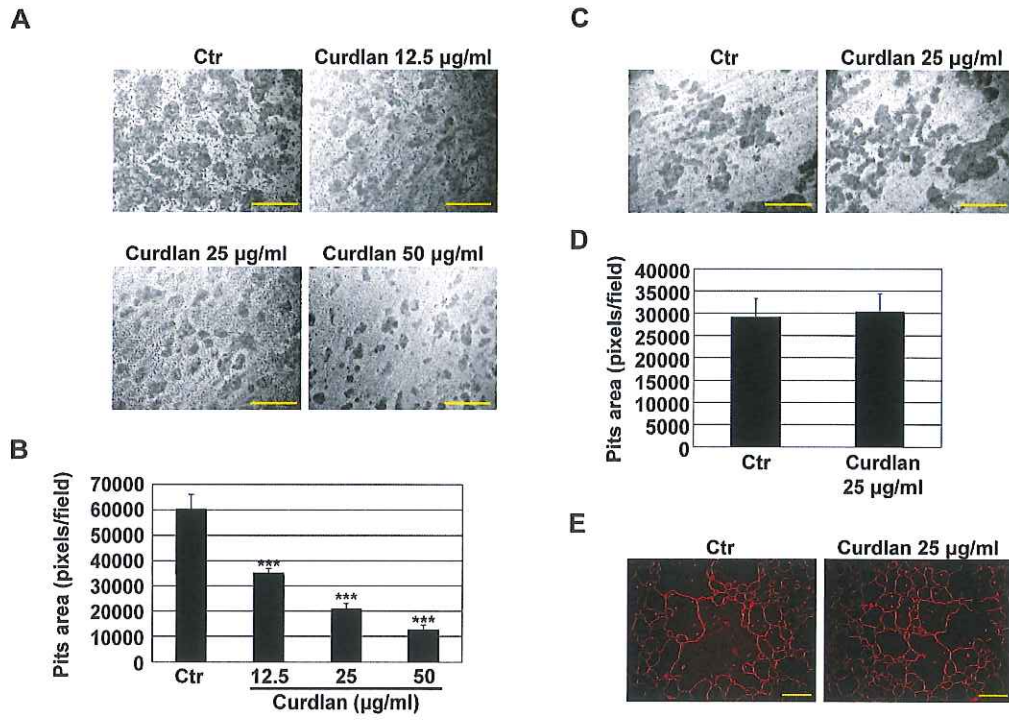
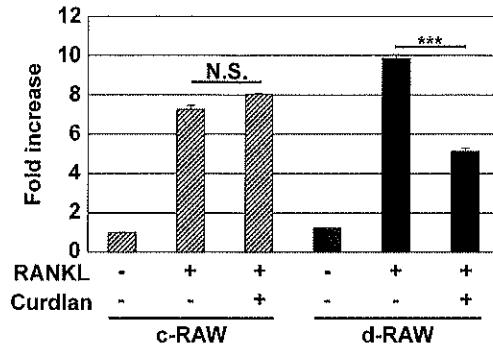
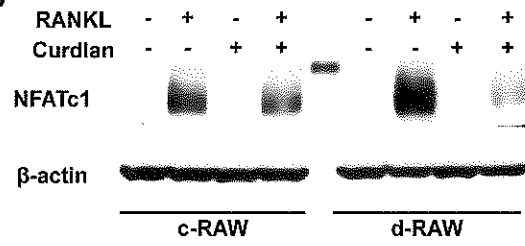


Figure 6

A



B



C

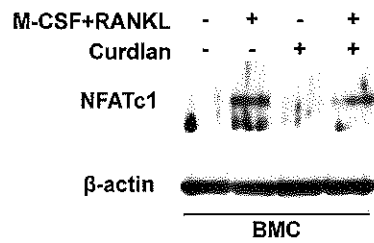


Figure 7

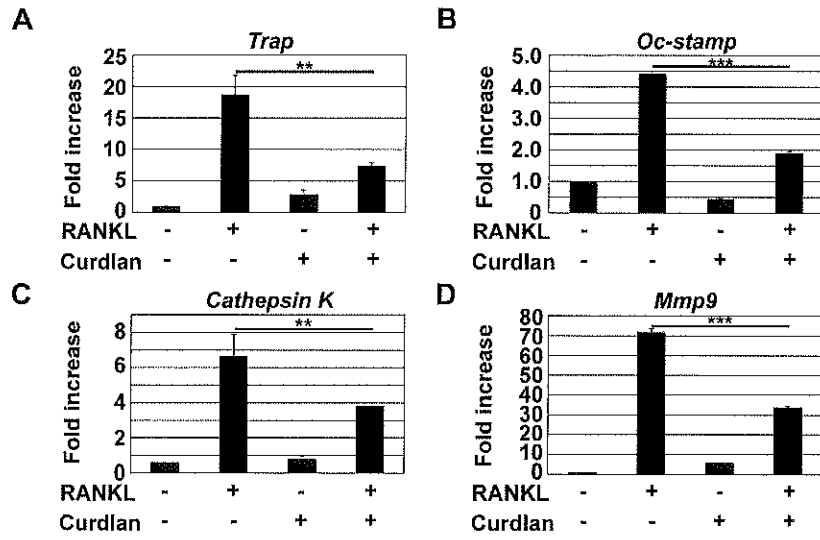


Figure 8

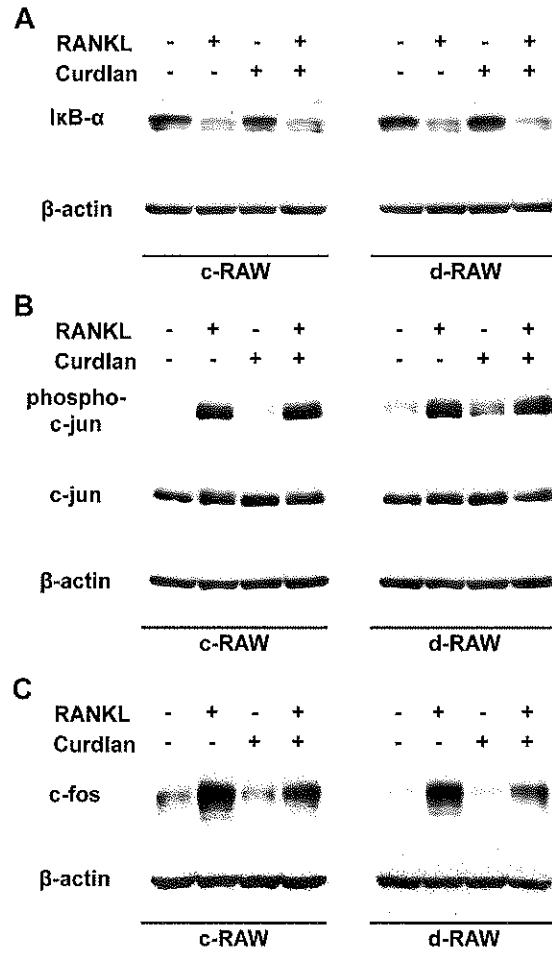


Figure 9

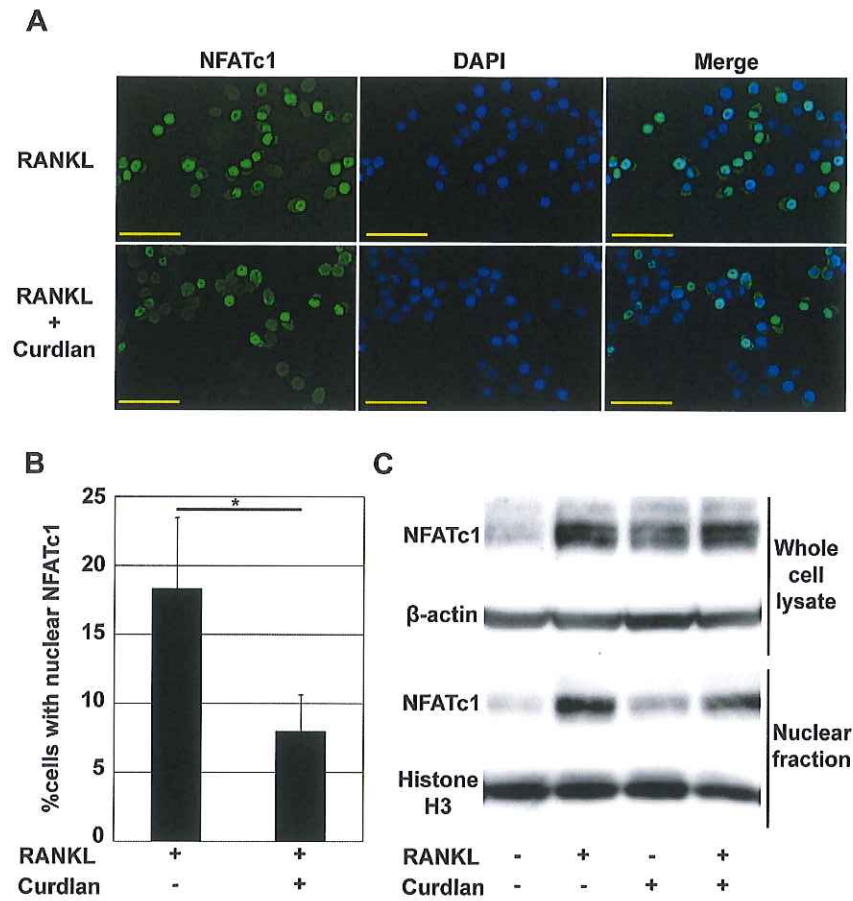


Figure 10

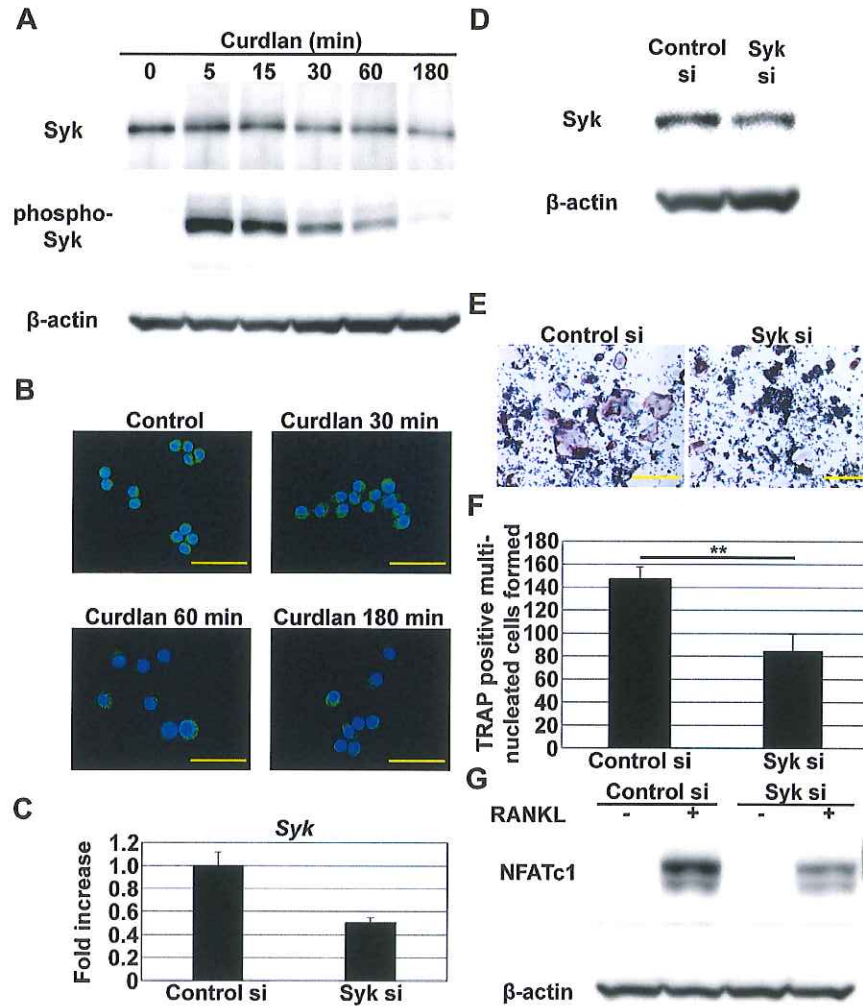


Figure 11

